Available online at www.sciencedirect.com
SCIENCE DIRECT®
International Journal of Heat and Mass Transfer 48 (2005) 1797–1807
International Journal of HEAT and MASS TRANSFER
www.elsevier.com/locate/ijhmt

The field synergy (coordination) principle and its applications in enhancing single phase convective heat transfer

Z.Y. Guo [a,*], W.Q. Tao [b], R.K. Shah [c]

[a] Department of Engineering Mechanics, Tsinghua University, Beijing 100084, China
[b] State Key Laboratory of Multiphase Flow in Power Engineering, Xi'an Jiaotong University, Xi'an 710049, China
[c] Department of Mechanical Engineering, Rochester Institute of Technology, Rochester, NY, USA

Received 27 March 2004; received in revised form 11 November 2004
Available online 26 January 2005

Abstract

In this paper the concept of field synergy (coordination) principle is briefly introduced first, and then its numerical verification is presented. A dimensionless number, field synergy number *Fc*, is defined as an indication of the synergy degree between velocity and temperature field for the entire flow and heat transfer domain. It is found that for the ideal case, this number should equal one, and for most of the engineering heat transfer cases, its value is far from being equal to one, showing a large room for the heat transfer enhancement study. Then the applications of the principle are discussed, with focusing being paid on the application for developing new type of enhanced techniques. Three examples are provided to demonstrate the importance and feasibility of the field synergy principle.

1. Introduction

Since convection heat transfer has broad applications in various engineering areas, a large amount of studies have been conducted in the past decades to get the heat transfer correlations and to improve heat transfer performance for different cases. However, the conventional way to investigate convection heat transfer has been to first classify convection as internal/external flow, forced/natural convection, boundary layer flow/elliptic flow, rotating flow/non-rotating flow, etc., then to determine the heat transfer coefficient, *h*, by both theoretical and experimental methods, and the corresponding dimensionless parameter, Nusselt number *Nu*. The *Nu* can usually be expressed as various functions of the Reynolds number *Re* (or Grashof number *Gr*) and Prandtl number *Pr* and heat transfer surface geometries [1,2]. Thereby, there is no unified principle, which may generally describe the performance of different types of convection heat transfer, and consequently guide the enhancement of convection heat transfer. Various kinds of techniques have been used in the past for heat transfer enhancement. Among them are: (a) mixing the main flow and/or the flow in the wall region using rough surface, inserts, etc., (b) reducing the boundary layer thickness by using interrupted fin geometries or jet impingement, etc., (c) creating the rotational or secondary flow using swirl flow devices or duct rotation, etc., (d) raising the turbulence intensity with rough surfaces and turbulence promoters, etc. [3,4]. From the above short description, it can be seen that there are two disadvantages for the existing techniques of heat transfer

* Corresponding author.
E-mail address: demgzy@tsinghua.edu.cn (Z.Y. Guo).

0017-9310/$ - see front matter © 2005 Elsevier Ltd. All rights reserved.
doi:10.1016/j.ijheatmasstransfer.2004.11.007

Nomenclature

a_t	turbulent thermal diffusivity, m^2/s
c_p	specific heat, J/kg K
D	hydraulic diameter, m
f	friction factor, dimensionless
Fc	field coordination number, defined by Eq. (13), dimensionless
Gr	Grashof number, dimensionless
h	heat transfer coefficient, W/m^2 K
Int	the term with integral in Eq. (14), W
k	thermal conductivity, W/m K
L	length, m
$\vec{n}$	surface unit normal vector
Nu	Nusselt number, hD_h/k, dimensionless
Pr	Prandtl number, dimensionless
q	heat flux, W/m^2
$\dot{q}$	heat source, W/m^3
r	radius, m
Re	Reynolds number, dimensionless
S	arc length along boundary, m
St	Stanton number, dimensionless
T	temperature, K
$\overline{T}$	dimensionless temperature
U	velocity, m/s
$\overline{U}$	$U/U_¥$, dimensionless velocity
u, v, w	velocity components, m/s
x, y, z	Cartesian coordinates, m
$\overline{y}$	y/δ_t, dimensionless

Greek symbols

β	field synergy angle between U and ∇T, degree
δ_t	thermal boundary layer thickness, m
∇T	temperature gradient, K
$\nabla \overline{T}$	$\frac{\nabla T}{(T_\infty - T_w)/\delta_t}$, dimensionless
ρ	density, kg/m^3
Ω	domain

Subscripts

Int	integral
q	constant heat flux
m	average
T	constant wall temperature
w	value on the wall surface
x	based on length x
∞	value at great distance from a body

augmentation. First, it lacks a way to understand the inherent universal mechanism of various techniques of heat transfer enhancement. Second, a large additional flow resistance, hence the pumping power, is usually associated with the heat transfer enhancement techniques, which is not favorable for practical applications.

The present paper starts from a revisit to the mechanism of convective heat transfer, and then indicates that the heat transfer rate depends not only on the flow and temperature fields, but also on their synergy (coordination). The so-called field synergy (coordination) principle proposed by Guo et al. [5,6] is then reviewed and its applications in the development of enhanced heat transfer surfaces are presented. Consequently, we cannot have only a thorough understanding of the universal mechanism of various heat transfer enhancement techniques, but also can further develop novel heat transfer enhancement structures, which can enhance the heat transfer with a small or reasonable increase of the pumping power.

2. Convective heat transfer mechanism

Consider an analog between convection and conduction, convection heat transfer is essentially the heat conduction with fluid motion [7]. Consider a steady, 2-D boundary layer flow over a cold flat plate at zero incident angle, as shown in Fig. 1(a). The energy equation is

$$\rho c_p = \left(u\frac{\partial T}{\partial x} + v\frac{\partial T}{\partial y}\right) = \frac{\partial}{\partial y}\left(k\frac{\partial T}{\partial y}\right) \tag{1}$$

The energy equation for conduction with a heat source between two parallel plates at constant but different temperatures as shown in Fig. 1(b) is

$$-\dot{q} = \frac{\partial}{\partial y}\left(k\frac{\partial T}{\partial y}\right) \tag{2}$$

From Eqs. (1) and (2) and Fig. 1, it can be seen that the convection term in the energy equation for the boundary layer flow corresponds to the heat source term

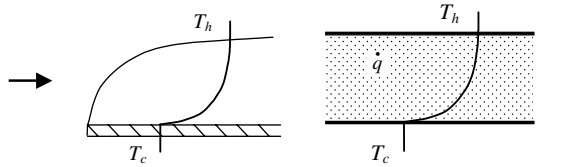

(a) Laminar boundary layer **(b)** conduction with a heat source

Fig. 1. Temperature profiles for (a) laminar boundary layer flow over a flat plate, and (b) conduction with a heat source between two parallel plates at different constant temperatures.

in the conduction equation. The difference is that the "heat source" term in convection is a function of the fluid velocity. The presence of heat sources leads to increased heat flux at the boundary for both the conduction and convection problems. The integral of Eq. (1) over the thickness of the thermal boundary layer is

$$\int_0^{\delta_t} \rho c_p \left(u\frac{\partial T}{\partial x} + v\frac{\partial T}{\partial y} \right) \mathrm{d}y = -k\left.\frac{\partial T}{\partial y}\right|_w = q_w \tag{3}$$

where δ_t is the thermal boundary layer thickness.

Eq. (3) indicates that the wall heat flux is equal to the overall strength of the heat sources inside the thermal boundary layer. This implies that the convection heat transfer can be enhanced by increasing the quantity of the integral of the convection terms (heat sources) over the thermal boundary layer.

3. Field synergy principle

3.1. Field synergy and heat transfer performance

Eq. (3) can be rewritten with the convection term in vector form as:

$$\int_0^{\delta_t} \rho c_p (u \cdot \nabla T)\mathrm{d}y = -k\left.\frac{\partial T}{\partial y}\right|_w = q_w \tag{4}$$

From Eq. (4) it can be seen that for a certain flow rate and temperature difference between the wall and the incoming flow, the wall heat flux increases with the decreasing of the included (intersection) angle between the velocity and temperature gradient/heat flow vectors. Eq. (4) is also valid for laminar duct flow if the upper limit of the integral is the duct radius.

With the following dimensionless variables for the boundary layer flow,

$$\overline{U} = \frac{U}{U_\infty}, \quad \nabla\overline{T} = \frac{\nabla T}{(T_\infty - T_w)/\delta_t} \tag{5}$$

Eq. (4) can be written in the dimensionless form

$$Nu_x = Re_x Pr \int_0^1 (\overline{U} \cdot \nabla\overline{T})\mathrm{d}\bar{y} \tag{6}$$

Eq. (6) gives us a more general insight on convective heat transfer. It can be seen that there are two ways to enhance heat transfer: (a) increasing Reynolds or/and Prandtl number; which is well known in the literature; (b) increasing the value of the dimensionless integration.

The vector dot product, $\overline{U} \cdot \nabla\overline{T}$ in the dimensionless integration in Eq. (6) can be expressed as

$$\overline{U} \cdot \nabla\overline{T} = |\overline{U}||\nabla\overline{T}|\cos\beta \tag{7}$$

where β is the included angle between the velocity vector and the temperature gradient (heat flow vector). Eq. (7) shows that in the convection domain there are two vector fields, U and ∇T, or three scalar fields, $|U|$, $|\nabla T|$ and $\cos\beta$. Hence, the value of the integration or the strength of the convection heat transfer depends not only on the velocity, the temperature gradient, but also on their synergy.

Thus the principle of field synergy for the enhancement of convective heat transfer may be stated as follows: the better the synergy of velocity and temperature gradient/heat flow fields, the higher the convective heat transfer rate under the same other conditions. The synergy of the two vector fields or the three scalar fields implies that (a) the included angle between the velocity and the temperature gradient/heat flow should be as small as possible i.e., the velocity and the temperature gradient should be as parallel as possible; (b) the local values of the three scalar fields should all be simultaneously large, i.e., larger values of $\cos\beta$ should correspond to larger values of the velocity and the temperature gradient; (c) the velocity and temperature profiles at each cross section should be as uniform as possible. Better synergy among such three scalar fields will lead to a larger value of the Nusselt number.

3.2. Extension of field synergy principle

Most convective heat transfer problems encountered in engineering are of elliptic type, therefore the extension of the field synergy concept to elliptic cases will be of great importance. Tao et al. [8] proved that this finding is also valid for elliptic flows. Consider a typical elliptic convective heat transfer case—fluid flow and heat transfer over a backward step, as shown in Fig. 2. The solid walls are of constant temperature T_w, and fluid with temperature T_f flows into the domain.

The integration of the heat sources (i.e., the convective term) over the domain is equal to the heat flux at the wall surfaces, if the axial heat conduction in the fluid can be neglected (for flow with Peclet number larger than 100 [9]), as indicated in Eq. (8) by using the Gauss theorem for reduction of the integral dimension.

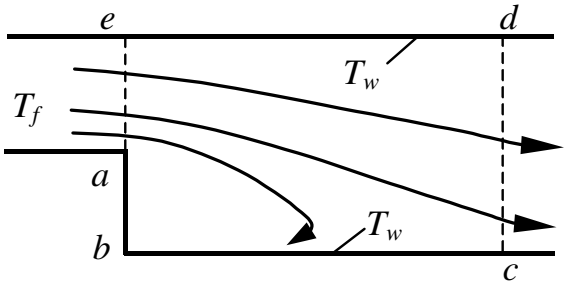

Fig. 2. Flow and heat transfer over a backward facing step.

$$\int\int_{\Omega_{abcdea}} \rho c_p (U\cdot\nabla T)\mathrm{d}x\,\mathrm{d}y = \int_{abc} \vec{n}\cdot k\nabla T\,\mathrm{d}S + \int_{de} \vec{n}\cdot k\nabla T\,\mathrm{d}S = q_{w,abc} + q_{w,de} \tag{8}$$

It is clear that a better synergy (i.e., decreasing the included angle between the velocity vector and the temperature gradient) will make the integration value larger, i.e., enhancing the heat transfer. It should be noted that even for fluid flow whose Peclet number is less than 100, the reduction of the included angle between the velocity and the temperature gradient can also enhance heat transfer, though the effect is not so significant as for the case with a larger Peclet number. Thus either for parabolic flows or for elliptic flows, the field synergy principle stated above is valid. The extension of above discussion to three-dimensional cases is very straightforward, and will not be discussed here for simplicity.

For turbulent duct flow, if axial heat conduction in the fluid can be neglected, the time-mean energy equation is:

$$\rho c_p\left(\frac{\partial T}{\partial x} + v\frac{\partial T}{\partial y}\right) = \frac{\partial}{\partial y}\left((k+\rho c_p a_t)\frac{\partial T}{\partial y}\right) \tag{9}$$

where a_t is the turbulent thermal diffusivity.

The integration of Eq. (9) over the entire domain and the use of the Gauss theorem lead to

$$\iiint_{\Omega}\rho c_p(U\cdot\nabla T)\mathrm{d}\Omega = \oint_{w}(k+\rho c_p a_t)\frac{\partial T}{\partial y} \tag{10}$$

Since a_t is equal to zero at the wall surface, we have

$$\iiint_{\Omega}\rho c_p(U\cdot\nabla T)\mathrm{d}\Omega = \oint_{w} k\frac{\partial T}{\partial y}\,\mathrm{d}S = q_w \tag{11}$$

Eq. (11) indicates that the wall heat flux for turbulent duct flow, as with laminar flow, can be expressed by the overall strength of the heat sources in the entire domain of duct. Hence, the field synergy principle can also be applied to turbulent duct flows and heat transfer. In Table 1 the calculated Nusselt numbers based on Eq. (6) (Nu_{int}) are compared with values based on the experimental correlation (Nu_{exp}), Eq. (12), which is the well-accepted Gnielinski correlation for the turbulent heat transfer in tubes or ducts [10]. It can be seen that the relative discrepancies between the Nu_{int} and Nu_{exp} are all less than 4%.

$$Nu = \frac{(f/8)(Re-1000)Pr}{1+12.7(f/8)^{1/2}(Pr^{2/3}-1)} \tag{12}$$

In the calculation of Nusselt number by Eq. (6), the dimensionless velocity and temperature distributions are obtained from numerical simulation.

3.3. Numerical verification of field synergy principle

For some heat transfer surfaces, numerical computations were carried out to obtain the integral over the whole computation domain and the average Nusselt number for the configuration studied. For the simplicity of presentation, the integral of the convective term over the entire domain (the most left term of Eq. (4)) will be represented by 'Int'. All computations were conducted by finite volume method, with CLEAR algorithm to deal with the linkage between velocity and pressure [11]. The flows computed were assumed to be in steady state. A number of two-dimensional fluid flow and heat transfer cases have been simulated [8,13], and for the simplicity of presentation, only one case is presented below. It is of periodic fully developed convective heat transfer of turbulent air flow, and the cyclic average Nusselt number was determined for the constant wall temperature situation. The details of the numerical procedure, especially the implementation of the periodically boundary conditions are provided in [12], where basically the same computer code was used and good agreement between the numerical predictions and available test data was obtained.

The turbulent flow across a 2-D parallel and staggered plates is shown in Fig. 3. The low-Reynolds number k–ε turbulence model was adopted. To implement the low-Re k–ε model, a very fine grid mesh is used adjacent to the plate surface. The mesh size is then gradually expanded away from the surface. The first near-wall grid point is located well within the laminar sublayer

Table 1
Comparison of the current results with standard values (Pr = 7.0)

Type	Boundary condition	Re	Nu_{int} Eq. (6)	$Nu_{exp}\,\frac{q_w}{(T_w-T_m)}\cdot\frac{D}{k}$	$\frac{Nu_{int}}{Nu_{exp}}$
Circular tube	Isothermal	20,000	151.4	157.0	0.967
		40,000	254.5	264.1	0.964
Circular tube	Constant flux	20,000	151.9	155.1	0.964
		40,000	254.2	264.4	0.961
Square tube	Isothermal	20,000	142.7	147.3	0.967
		40,000	256.9	248.1	0.966

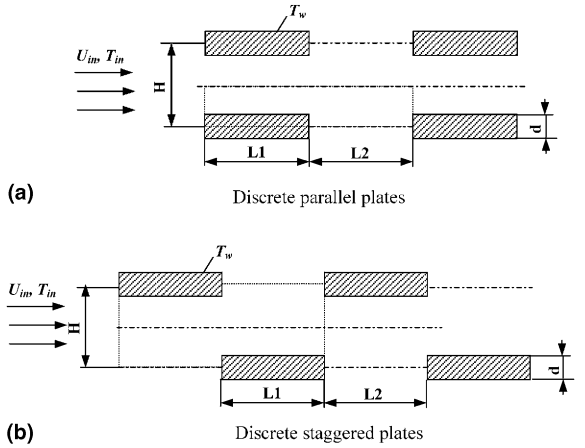

Fig. 3. Models of discrete plates. (a) Discrete parallel plates; (b) discrete staggered plates.

($y^+ = 0.1$) for all of the computations. The number of grids outside the laminar sublayer is always lager than 85. Grid independency tests are performed to ensure the grid-independent solution. A grid system of 304×92 is adopted for all computations. The variation of the integration with *Re* and the plate averaged Nusselt numbers are presented in Fig. 4(a) and (b). To reveal the variation trend of the included angle between velocity and temperature gradient, a domain averaged included angle was defined as follows:

$$\beta_m = \sum \cos^{-1}\left(\frac{\vec{u}\cdot \mathrm{grad}\, t}{|\vec{u}||\mathrm{grad}\, t|}\right)\frac{\Delta V}{V} \tag{13}$$

The domain averaged included angles between velocity and temperature gradient for the two series of plates are provided in Fig. 4(c). As can been there, the present numerical results agree well with the field synergy principle.

3.4. Field synergy number

In the above example, we take the domain averaged included angle as the indication of field synergy for the configurations studied. It should be noted that this indication has some limitation in the sense that if the local included angle is small and the local velocity and temperature gradient are also small, then the local good synergy does not make great contribution to the enhancement of the convective heat transfer. As indicated above, the most favorable case is that a small included angle is accompanied by large velocity and temperature gradients. The effect of such ideal case can be reflected from the final results—the integral of the convection term over the entire domain, for which the dimensionless expression can be obtained from Eq. (6) as follows:

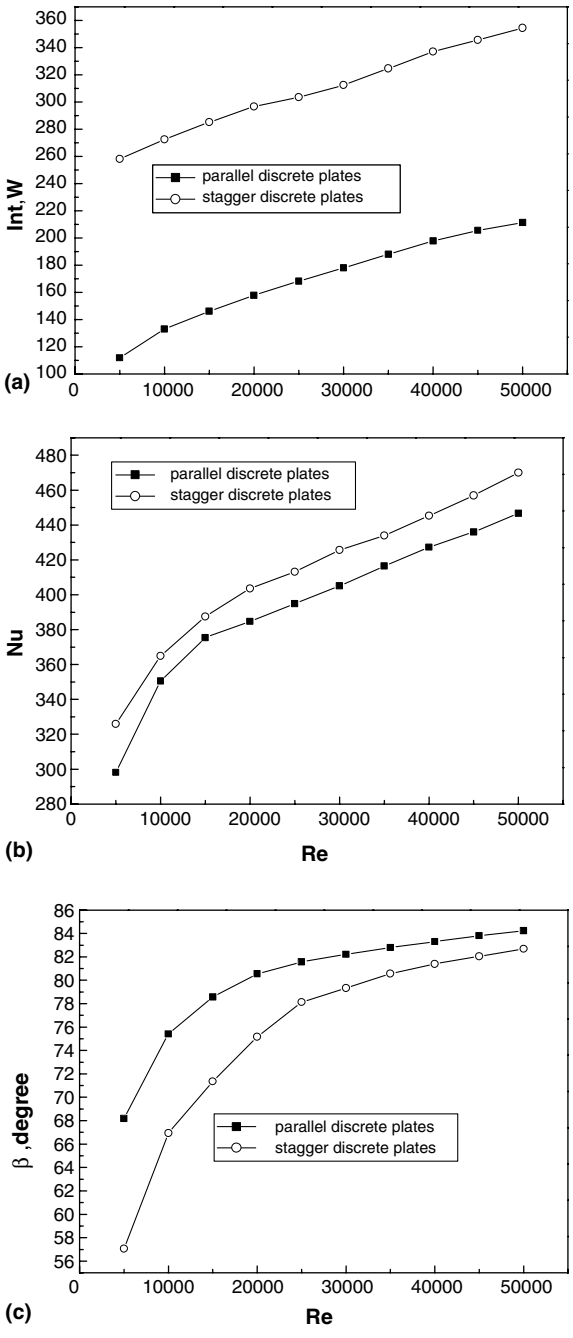

Fig. 4. Turbulent heat transfer characters across discrete plates. (a) Variation of Int with Reynolds number; (b) variation of *Nu* with Reynolds number; (c) variation of β with Reynolds number.

$$\int_0^1 (\overline{U}\cdot\nabla\overline{T})\mathrm{d}\bar{y} = \frac{Nu_x}{Re_x Pr} = Fc \tag{14}$$

where the dimensionless quantity *Fc* is introduced and is designated as the field synergy (coordination) number,

which represents the degree of synergy between the velocity and temperature gradient fields for the entire domain. *Fc* stands for the dimensionless heat source strength (i.e., the dimensionless convection term) over the entire domain, which physically is the indication of the degree of synergy between the velocity and temperature gradient fields. Its value can be anywhere between zero and one depending on the type of heat transfer surface. Note that *Fc* and the Stanton number [14], have identical formulas relating to the Nusselt number. However, $St = Nu/RePr$ is strictly the relationship between Stanton and Nusselt number and this equation is always valid (true) regardless the type of the flow and heat transfer surface geometry. *St* is an alternate to Nusselt for expressing dimensionless heat transfer coefficient for convective heat transfer over the heat transfer surface. To further illustrate the above physical interpretation of *Fc*, let assume that *U* and ∇T are uniform and the included angles, β, are equal to zero everywhere in the domain, then $Fc = 1$, and

$$Nu_x = Re_x Pr \tag{15}$$

For this ideal case the velocity and temperature gradient fields are completely coordinated and *Nu* reaches its maximum for the given flow rate and temperature difference. Thus the meaning of *Fc* should be clear. It should be noted that *Fc* is much smaller than unity for most practical convective heat transfer situation, as shown in Fig. 5. Therefore, from the view point of the field synergy principle, there is a large room open to the enhancement study for the convective heat transfer.

It is interesting to note that the field synergy principle gives us the direction to improve the convective heat transfer for a given condition (say, flow rate and temperature difference), such as the similarity theory indicates how to correlate the convective heat transfer data. However, the specific enhanced technique which can make better synergy for a given condition cannot obtained from the principle itself, just as the specific heat transfer correlation cannot be obtained from similarity theory. It is the individual research task to find such technique. This, of course, by no means implies that the principle is not useful, rather, it is very useful as will be demonstrated by a number of examples presented below.

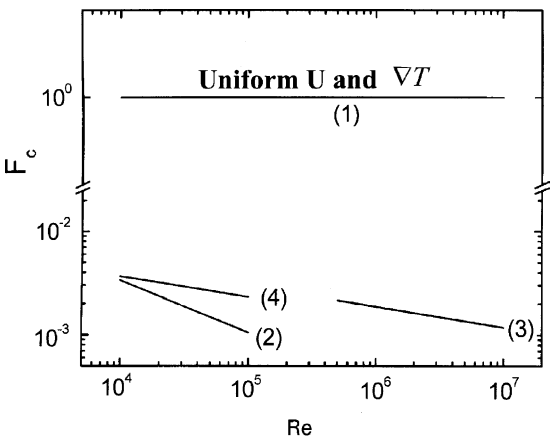

Fig. 5. Field coordination number for some convective heat transfer conditions.

3.5. Examples showing different degrees of synergy

In the following presentation, some experimental and numerical examples are provided to show different degrees of synergy between velocity and temperature gradient.

Zhao and Song [15] conducted an analytical and experimental study of forced convection in a saturated porous medium subjected to heating with a solid wall perpendicular to the flow direction as shown in Fig. 6(a). The heat transfer rate from the wall to the bulk fluid for such a heat transfer configuration had been shown to be described by the simple equation $Nu = RePr$ at low Reynolds number region as shown in Fig. 6(b), that is $Fc = 1$. Obviously, the complete coordination of the velocity and heat flow fields provides the most efficient heat transfer mode as compared with any other convective heat transfer situations.

The flow and heat transfer across a single circular cylinder with rectangular fins was numerically studied in [16]. To numerically simulate the flow field around the cylinder between two adjacent fins three-dimensional body fitted coordinates were adopted. The tube wall was kept at constant temperature and the fin surface temperature was assumed to be equal to tube wall temperature. The flow across single cylinder was also simulated for comparison. Numerical results of isotherms and velocity vectors for flow over single smooth tube with $U = 0.02$ m/s are presented in Fig. 7(a) and (b), from which it can be observed that over most part of the computational domain (except for upstream region where the isotherms are nearly vertical), the velocity and the local temperature gradient are nearly perpendicular each other, leading to a large field synergy angle. The synergy angle distribution is provided in Fig. 7(c). The average synergy angle of the whole domain is 61.7°. For the finned tube at the oncoming flow velocity of 0.06 m/s, the fluid isotherms and the flow velocity at the middle plane between two adjacent fin surfaces are presented in Fig. 8(a) and (b). It can be clearly observed that the attachment of fin to the tube surface greatly changes the orientation of the temperature isotherms as almost vertical so that the temperature gradient is in almost horizontal direction. The result is that the

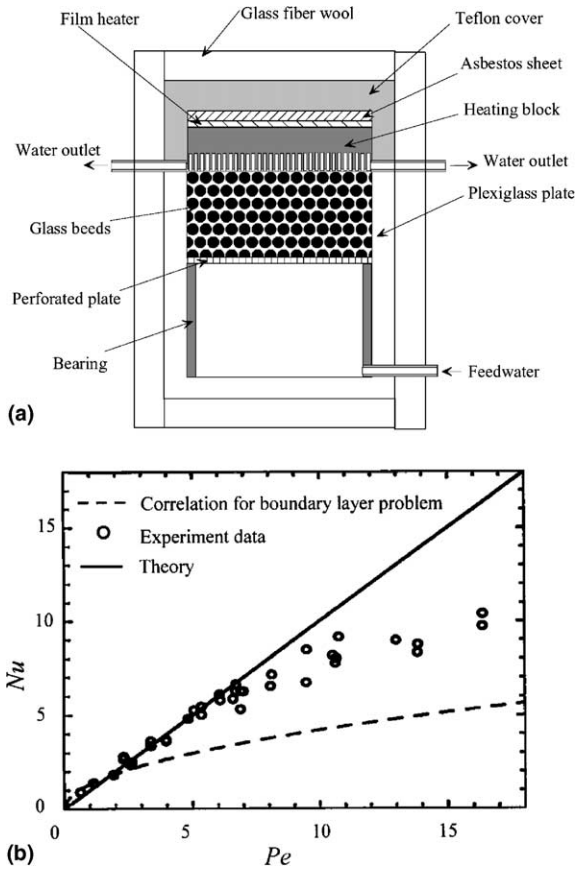

Fig. 6. Test section and Nu vs Pe for forced convection in a saturated porous medium; (a) test section; (b) Nu versus Pe for the wall.

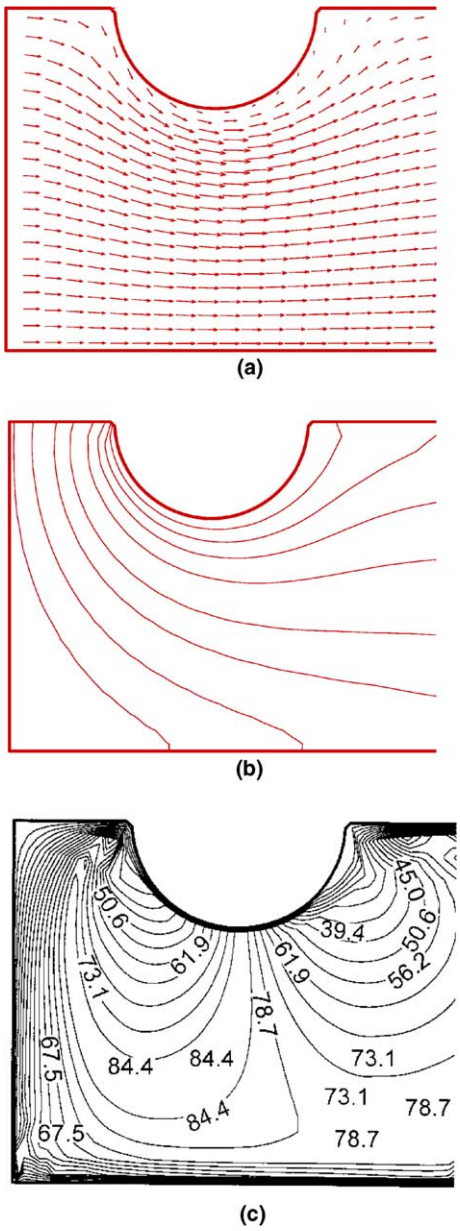

Fig. 7. Numerical results of velocity vectors, isotherms and included angles for flow over single tube ($U = 0.02$ m/s); (a) velocity vectors; (b) isotherms; (c) included angle distribution.

velocity and temperature gradient are almost parallel and thus in good synergy. The local included angle distribution is shown in Fig. 8(c), and the average included angle is now reduced to 23.6°. Computational results further reveal that in the region of very low velocity (for the case studied, the oncoming flow velocity less than 0.08 m/s), the average finned tube heat transfer coefficient varies almost linearly with the flow velocity, once again showing a case where the local velocity and temperature gradient is almost parallel everywhere.

4. Applications of field synergy principle in developing enhanced heat transfer surfaces

The field synergy principle has two types of applications. First it can facilitate to have a better understanding of known heat transfer phenomena or experimental results; Second, and more important, is to guide the development of novel enhanced heat transfer structures. In the following, two examples will be provided to show the first type of application and then focus will be paid to the second type of application.

It is well known that $Nu_q = 4.36$ for the fully developed laminar tube flow with the constant heat flux boundary condition, while $Nu_T = 3.66$ for the isothermal boundary condition. Our numerical results have shown that such a difference lies in the different included angle between U and ∇T for the two thermal boundary conditions.

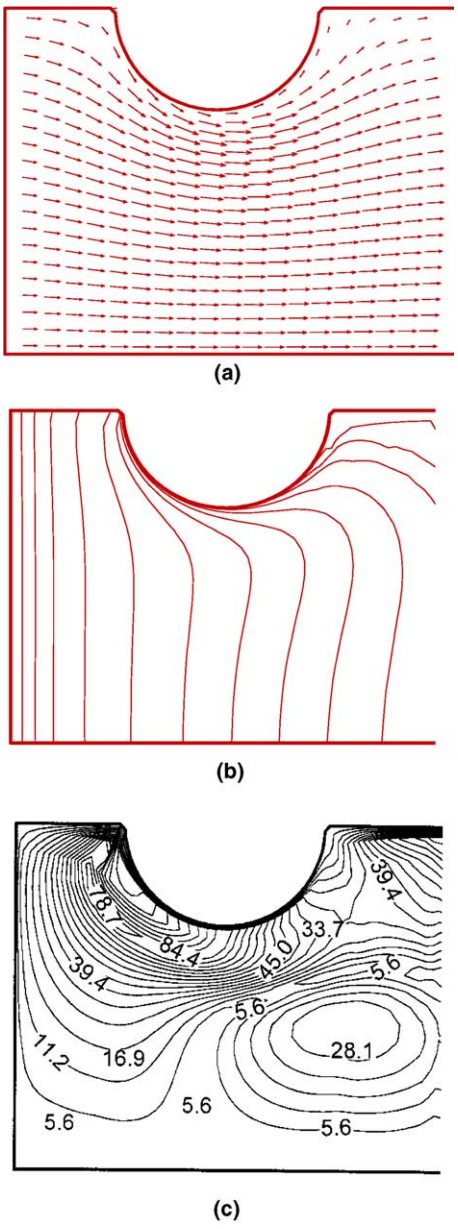

Fig. 8. Velocity vectors, isothermals and included angle distributions for flow over finned tube ($U = 0.06$ m/s); (a) velocity vectors; (b) isotherms; (c) included angle distribution.

Kang and Kim found by experiments that for the slotted fin surface the locations of the strips has great effect on the heat transfer and friction factor characteristics [17]. For the same number of strips, they found that the performance of the slotted fin surface for which the strips are located in the rear part of the fin is better than that in which the strips are located in the front part. Numerical simulation conducted by Qu et al. [18] found that the domain averaged synergy angle of the fin with strips located in the rear part is smaller than with strips positioned in the front part.

Now attention is turned to the development of new types of enhanced heat transfer surfaces by application of the field coordination principle. There are several ways to improve the synergy.

4.1. Variation of the velocity field

The velocity field in the duct flow can be varied by changing the duct configuration. For example, vortices occur when the flow goes through a specially designed alternatively twisted elliptic tube, as shown in Fig. 9(a) [19]. Fig. 9(b) gives the comparison results for the Nusselt number and friction factor between the test results for water and lubricating oil of the enhanced tube (denoted by Nu_e and f_e) and a smooth circular tube (denoted by Nu_s and f_s). It can be seen that a great enhancement can be made with a reasonable increase in the friction, and for the laminar flow case, the ratio of heat transfer enhancement is even much larger than that of the friction factor increase. Numerical results shown in Fig. 9(c) reveals that at each cross section there are several vortices which significantly improve the synergy between the velocity and the temperature field. From Fig. 9(c), it can be seen that at the locations where isotherms crossly intersected by the flow velocities the synergy is improved. For a straight elliptic tube there is no such vortex formed in the cross section and the synergy between velocity and temperature field is much worse, and hence the heat transfer.

4.2. Improved the uniformity of the temperature profiles

Inserts composed of sparse metal filaments are used in a circular tube to increase the uniformity of the temperature profile, which improves the field synergy between the velocity and heat flow fields. The filaments are normal to the tube wall as shown in Fig. 10(a) and (b) and thin enough to produce only slight additional increases in the pressure drops. Such kind of fins is neither for surface extension, nor for disturbance promotion, but for improvement of field synergy (coordination). Experimental results for this novel device are plotted in Fig. 10(c) [20]. The performance evaluation criteria (PEC), defined as $(Nu/Nu_0)/(f/f_0)1/3$, represents the heat transfer enhancement for a given pumping power, where the reference case for Nu_0 and f_0 is the fully developed laminar tube flow. Compared with most conventional enhanced tubes with air as the working medium in which the performance values usually less than 2 [3], this enhanced tube based on the principle of field-coordinated enhancement has performance values much larger than 2 at Re ranging from 200 to 3500.

(a)

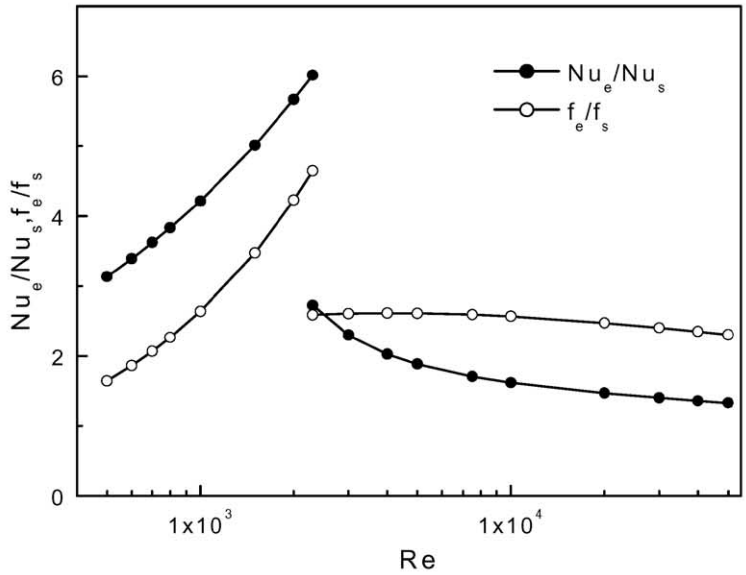

(b)

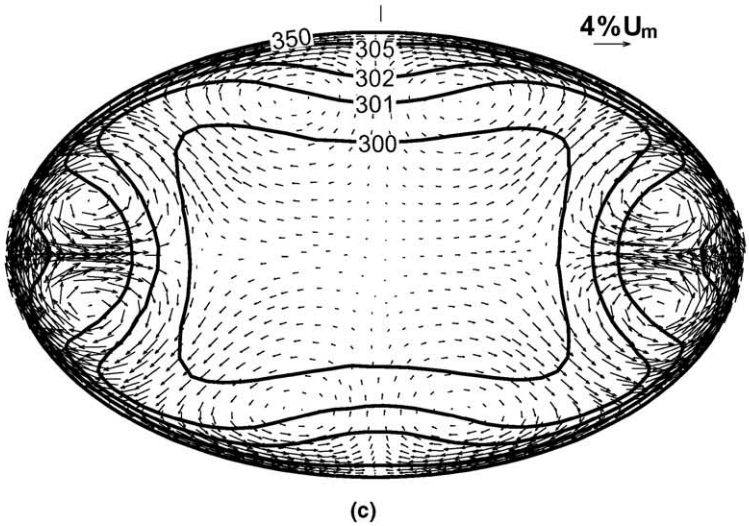

(c)

Fig. 9. Alternating elliptic axis tube and its heat transfer characters ($Re = 2 \times 10^4$). (a) Alternating elliptical axis tubes; (b) comparison of alternating elliptical axis tube with smooth tube; (c) velocity and temperature fields simulation in the cross section.

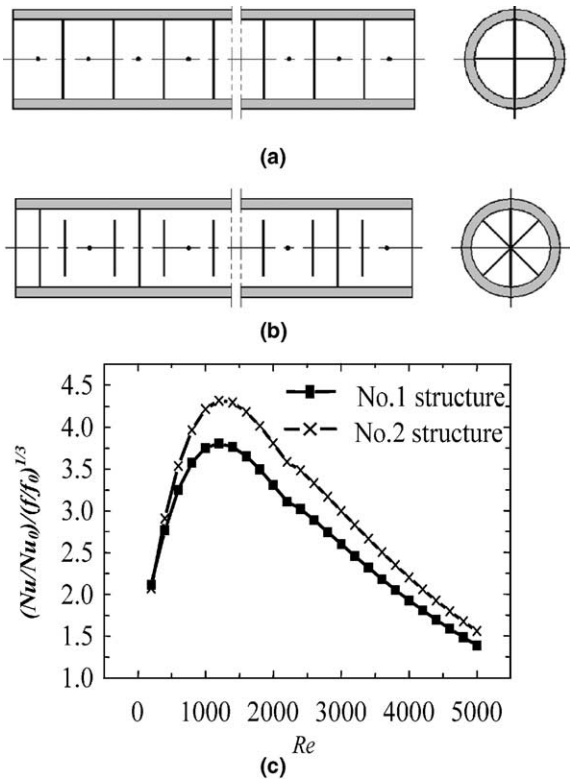

Fig. 10. Experimental results for tube with metal filament inserts. (a) Structure 1; (b) structure 2; (c) comparison of heat transfer performance.

4.3. Adjust the locations of the strips in the fin surface

For air flow across three-row tube finned surface some specially designed parallel slotted fin surfaces are numerically investigated with the strips position according to a rule called "front sparse and rear dense" as shown in Fig. 11(a) [21]. Numerical results show that such kind of enhanced surface has much higher heat transfer performance than that of a plain fin surface. Fig. 11(b) presents a comparison of the Nusselt numbers under the identical pumping power constraint. The superior performance of the parallel slotted fin studied is very obvious. Such special slotted fin surface is designed using the field synergy principle: the locations of the strips are found by numerical analysis such that the domain averaged synergy angle is almost the smallest. Such nearly optimum configuration was searched through several arrangements of the strips along the flow direction. Fig. 11(c) provides the domain average intersection angle of the plain plate fin and the slotted fin with strips arranged according to the rule of front sparse and rear dense. It can be seen that the intersection angle of the proposed slit fin is much less than of the plain plate fin, indicating a better synergy of the slotted fin surface.

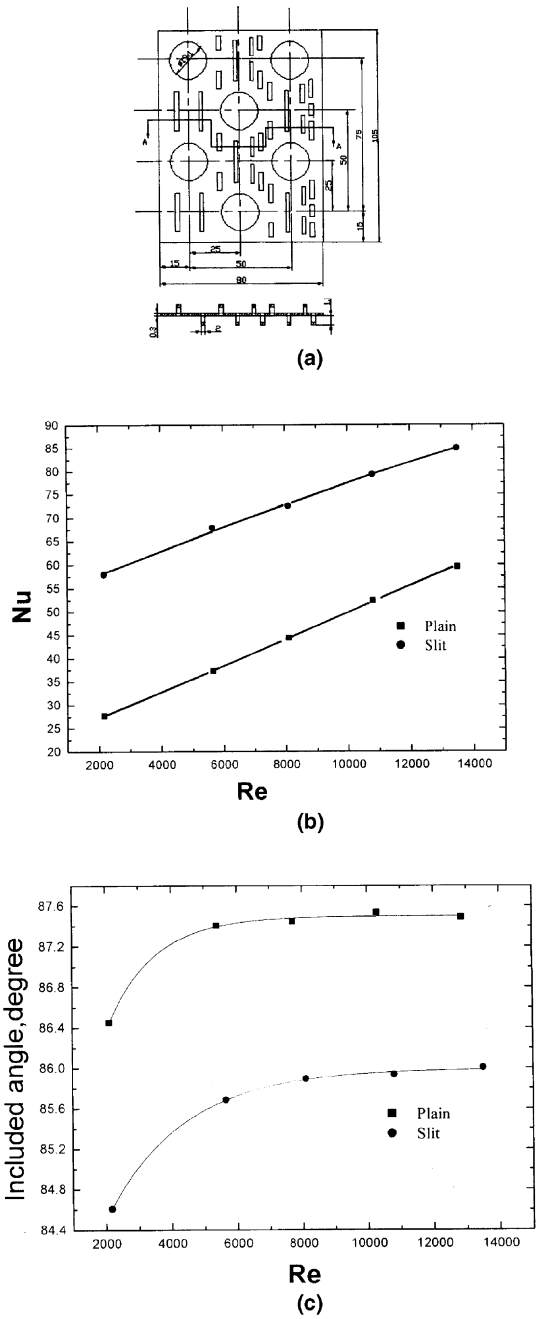

Fig. 11. Performance comparisons of slotted fin and plain plate fin. (a) Front sparse and rear dense distribution of strips; (b) comparison of *Nu* under identical pressure drop; (c) computation of domain averaged intersection angle.

5. Concluding remarks

(1) The field synergy principle indicates that improving synergy for the velocity and temperature gradient/heat flow fields can markedly enhance heat transfer

with less increased flow resistance, which will find widespread applications in many engineering fields.

(2) The field synergy number, Fc, measures the synergy degree of the fluid velocity and temperature gradient/heat flow fields for the entire flow domain. According to the field synergy principle the upper limit of convection heat transfer for a fixed flow rate and a given temperature difference is $Fc = 1$ or $Nu = RePr$. Therefore, a large room of improvement opens to most of the convective heat transfer processes encountered in engineering practice where the value of Fc is much less than unity.

(3) The field synergy principle can be used enhancing our understanding of some well-known heat transfer phenomena and experimental results. It also provide very useful rule to improve surface structure for a better heat transfer performance.

(4) There are several ways to improve the synergy between the velocity and temperature gradient/heat flow fields, including varying the velocity and temperature boundary conditions, varying the velocity field in duct flows, the use of specially designed inserts, tubes, and fins, and the adoption of parallel slotted fin surface with front sparse and rear dense strip position.

Acknowledgments

This work was financially supported by the State Key Basic R&D Program of China (Grant no. G20000263). Our thanks also go to Mr. Z.G. Qu and Y. Wu and Ms Z. Li for their help in re-computing some cases.

References

[1] W.M. Rohsenow, J.P. Hartnett, E.N. Ganic, Handbook of Heat Transfer, second ed., McGraw-Hill, New York, 1985, Chapters 6,7, and 8.

[2] L.C. Burmeister, Convective Heat Transfer, John Wiley & Sons, New York, 1983, 207.

[3] R.L. Webb, Principles of Enhanced Heat Transfer, John Wiley & Sons, New York, 1994, pp. 3–11.

[4] A.E. Bergles, Application of Heat Transfer Augmentation, Hemisphere Pub Co., London, 1981.

[5] Z.Y. Guo, D.Y. Li, B.X. Wang, A novel concept for convective heat transfer enhancement, Int. J. Heat Mass Transfer 41 (1998) 2221–2225.

[6] Z.Y. Guo, S. Wang, Novel concept and approaches of heat transfer enhancement, in: P. Cheng (Ed.), Proceedings of Symposium on Energy and Engineering, vol. 1, Begell House, New York, 2000, pp. 118–126.

[7] F.M. White, Heat Transfer, Addison-Wesley Publishing Company, New York, 1984, p. 6.

[8] W.Q. Tao, Z.Y. Guo, B.X. Wang, Field synergy principle for enhancing convective heat function—its extension and numerical verification, Int. J. Heat Mass Transfer 45 (2002) 3849–3856.

[9] W.M. Kays, M.E. Crawford, Convective Heat and Mass Transfer, McGraw-Hill Book Company, New York, 1980, p. 107, 246.

[10] V. Gnielinski, New equations for heat and mass transfer in turbulent pipe and channel flows, Int. Chem. Eng. 16 (1976) 359–368.

[11] W.Q. Tao, Z.G. Qu, Y.L. He, A novel segregated algorithm for incompressible fluid flow and heat transfer problems-CLEAR (coupled and liked equations algorithm revised), Part I: Mathematical formulation and solution procedure, Numer Heat Transfer, Part B 45 (2004) 1–18.

[12] L.B. Wang, W.Q. Tao, Heat transfer and fluid flow characteristics of plate-array aligned at angles to the flow direction, Int. J. Heat Mass Transfer 38 (1995) 3053–3063.

[13] M. Zeng, W.Q. Tao, Numerical verification of the field synergy principle for turbulent flow, J. Enhanced Heat Transfer 11 (2004) 451–457.

[14] F.P. Incropera, D.P. DeWitt, Fundamentals of Heat and Mass Transfer, John Wiley & Sons, New York, 2002, p. 356.

[15] T.S. Zhao, Y.J. Song, Forced convection in a porous medium heated by a permeable wall perpendicular to flow direction: analyses and measurements, Int. J. Heat Mass Transfer 44 (2001) 1031–1037.

[16] W.Q. Tao, Y.L. He, Q.W. Wang, Z.G. Qu, F.Q. Song, A unified analysis on enhancing single phase convective heat transfer with field synergy principle, Int. J. Heat Mass Transfer 45 (2002) 4871–4879.

[17] H.C. Kang, M.H. Kim, Effect of strip locations on the airside pressure drop and heat transfer in strip fin-and-tube heat exchanger, Int. J. Refrig. 22 (1999) 302–312.

[18] Z.G. Qu, W.Q. Tao, Y.L. He, 3D Numerical simulation on laminar heat transfer and fluid flow characteristics of slitted fin surfaces-Investigation of strip location effect, ASME J. Heat Transfer 126 (2004) 697–707.

[19] J.A. Meng, Enhanced heat transfer technology of longitudinal vortices based on field-coordination principle and its application. PhD. Thesis, Tsinghua University, Beijing, China, 2003.

[20] S. Wang, Z.X. Li, Z.Y. Guo, Novel concept and device of heat transfer augmentation, in: Proceedings of the Eleventh International Heat Transfer Conference, vol. 5, 1998, pp. 405–408.

[21] Y.P. Cheng, Z.G. Qu, W.Q. Tao, Y.L. He, Numerical design of efficient slotted fin surface based on the field synergy principle, Numer. Heat Transfer, Part A 45 (2004) 1–22.